Steir. Beitr. z. Hydrogeologie / 43 / Seiten 251–280 / Graz 1992

Porous Aquifer – Test Site Merdingen (Germany)

A. De Carvalho Dill, K. Gerlinger, T. Hahn, H. Hötzl, W. Käss, Ch. Leibundgut, P. Maloszewski, I. Müller, S. Oetzel, D. Rank, G. Teutsch, A. Werner

Content

1. Area of Investigation (A. De Carvalho Dill, H. Hötzl, W. Käss, I. Müller, D. Rank)

1.1. Location and Test Field Inventory

The test field Merdingen is situated in the Upper Rhine Valley, Southwest Germany, about 15 km northwest of Freiburg (Fig. 1.1). The test field is set up in

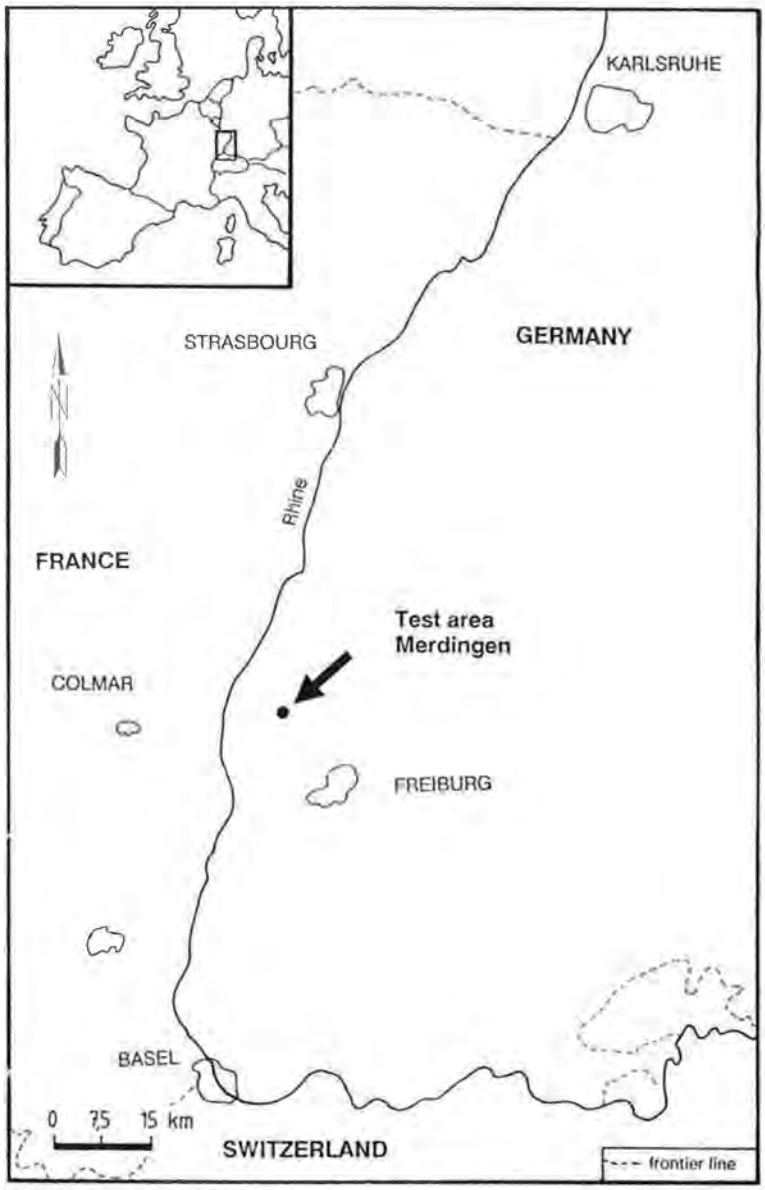

Fig. 1.1: Location of the test area Merdingen.

a gravelplain between the two mountains, the Kaiserstuhl in the NW and the Tuniberg in the S. In early historic time (Romans) the Rhine flew temporarily through the 2 km wide passage between this two elevations, while later on it has shifted its bed to the west side of the Kaiserstuhl (Fig. 1.2).

The test field of Merdingen comprises two well fields, which were drilled into the upper part of the gravel sequence for different hydraulic and hydrochemical studies of this porous aquifer. It has been in operation for 15 years. The ground water studies there were started within the frame of a research project founded by the German Research Foundation (DFG) in 1978. Later on it was used for different projects with increasing well inventory.

Today the test field consists of two more or less parallel fan shaped well sets with together 130 wells. The wells are dominantly flat wells with depths of less than 5 m. The groundwater level is situated in the average about 1.50 m below the surface, so that the wells penetrate only the uppermost 2 m of the about 20 m thick aquifer. The wells are made of rammed 1 1/2" steeltubes with perforation in the lower part (Fig. 1.3). Only five boreholes are penetrating the aquifer to a depth of 10 m, they are equipped with filters ranging from 1–2 m, 4–5 m and from 9–10 m.

The two fan shaped well sets are arranged with their axes in the ground water flow direction towards NE. In the well set A the observation wells are positioned along circular arches in a distance of 6.25 m, 12 m, 25 m, 50 m, 100 m and 200 m from the main injection well (Fig. 1.4). In the well set B with its main axis 40 m from the first one the observation wells are arranged in rows perpendicular to the axis.

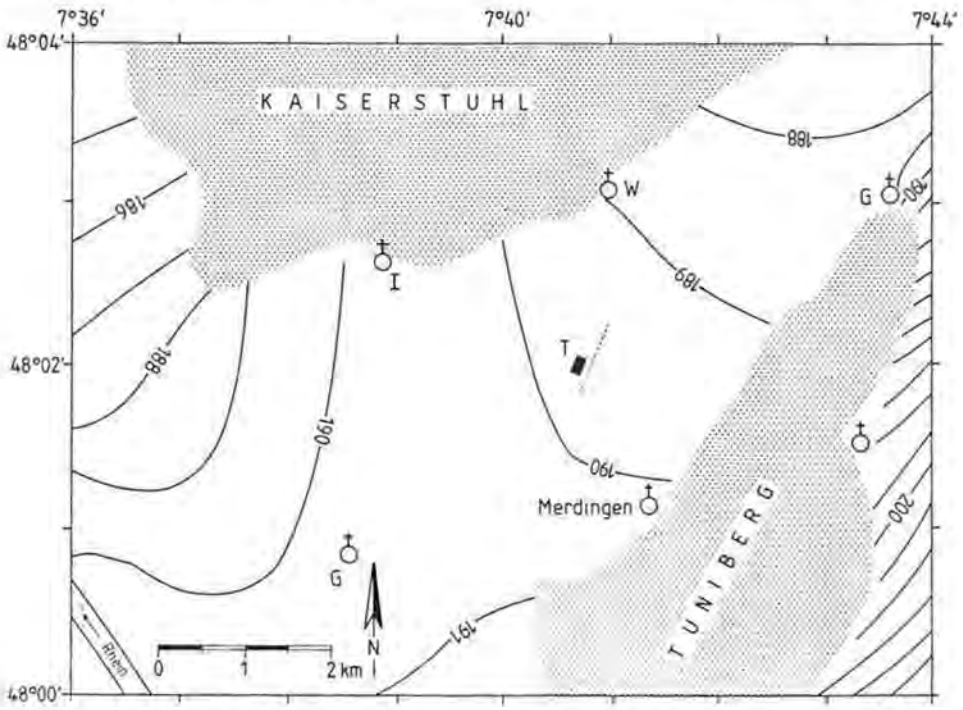

Fig. 1.2: Contours of the water table in the environment of the test field Merdingen (MELU + MWMV 1977). Dotted line: geoelectric measuring profile.

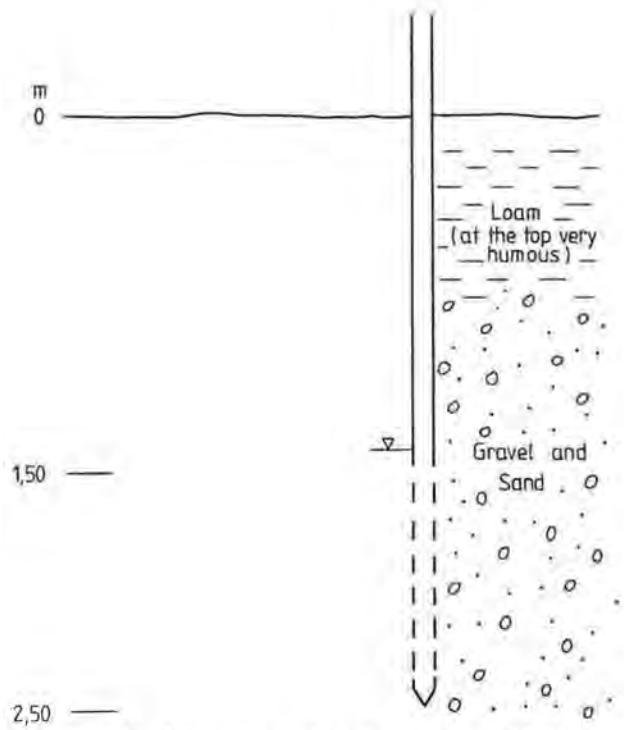

Fig. 1.3: Schematic design of the observation wells in the test field of Merdingen.

In connection with ATH tracing program at the test site of Merdingen only the well set A was used for a combined tracing experiment. This experiment was partly performed for the further evaluation and reinterpretation of the former 27 tracer tests, which have been carried out there since 1979.

No accompanying hydrogeological and hydrochemical investigations were done within the frame of this recent experiment. For the details of the former investigations the reader is refered to W. KÄSS (1988). Only additional geophysical surveying was carried out to get a better understanding of the aquifer heterogeneity (cf. chap. 1.4.).

The climatic conditions of the area around the test site are characterized by an annual average of temperature of 8.5° C and by precipitation of 650 mm. The vegetation at the site consists of a deciduous wood. Agricultural areas with mainly maize cultures begin 200 m upstream.

1.2. Geology and Hydrogeology

The Upper Rhine Valley is a Tertiary Rift System through which the Rhine river is flowing from S (Basel) to the N (Mainz–Frankfurt) only since the beginning of Quaternary. The graben basin is a strongly block faulted area, where at the more marginal parts small horst like structures, like the Tuniberg south of the test field, still rises above the young gravelplain. The elevation on the NW side of the test area, the Kaiserstuhl, is another relict of the graben development. It represents a volcanic torso mountain of Miocene age.

The young sediments filling of the basin was derived nearly exclusively from the graben flanks (Black Forest and Vosges) up to the Pliocene. Since the breakthrough of the Rhine river debris from the Alpine area has become dominant. The Quaternary sediments comprise in the lower part sandy and silty sequences, in the uper part mainly sand with gravels, which are separated by few silt and clay layers. The latter are responsible for the subdivision of the gravels into different aquifers.

The test site Merdingen refers to the uppermost unconfined aquifer. It is formed by the Late Pleistocene and Holocene gravels with a thickness there of about 20 m. Their hydraulic conductivity (k_f) amounts about 5×10^{-3} up to 2×10^{-4} m/s. These gravels are covered in the test area by a soil and clay layer of about 1 m.

The groundwater level is situated in a depth of about 1.5 m; its decline is directed towards NE with inclination of 0.5‰ obvious (Fig. 1.2). The decline is very low because of the location of the test area directly east of a valley water shed which is due to the shifting of the Rhine river to the W. During the time of observation from summer 1978 the lowest groundwater level in the test field was at 189.47 m a.s.l. on September 12th, 1991, the highest value at 190.87 m was observed on May 30th, 1983.

Wells for water supplies are at least 1,000 m off the test field and do not influence the water level there. Two small brooks are passing the test area in a distance of 500 m and about 1,000 m.

1.3. Hydrogeochemistry

The composition of the groundwater in the test field is typical for the groundwater in the alluvial sediments derived from the Alps. Due to the high amount of carbonate components it is characterized by the dominance of calcium and hydrogencarbonat with total amount of dissolved components of about 700 mg/l. Further components

Tab. 1.1: Hydrochemical datas for the groundwater in the testfield Merdingen.

Depth (m)	1–2	4–5	9–10	Rainwater
Temperature (°C)	12.0	12.2	11.9	
Conductivity (µS · cm^{-1}/20° C)	705	693	698	15.3
pH	7.19	7.19	7.24	6.91
Eh (mV)	509	514	529	
Hardness, total (meq/l)	7.51	7.44	7.44	
Na^+ (mg/l)	16.6	16.5	16.5	2.05
K^+ (mg/l)	2.11	2.58	2.37	2.28
Li^+ (µg/l)	4.7	4.9	8.6	
Sr^{2+} (µg/l)	271	266	275	
Cl^- (mg/l)	35.6	33.7	33.5	
NO_3^- (mg/l)	43	38	37	
SO_4^- (mg/l)	45.0	45.5	45.7	
O_2 (mg/l)	2.9	5.7	4.6	
O_2 (% saturation)	28	54	43	
CO_2 (mg/l)	20	22	22	
^3H (T.U.)	45.5	45.2	41.4	12.6
$\delta^{18}O$ (‰ SMOW)	–8.50	–8.56	–8.55	–11.41

are listed in tab. 1.1. A nearly equable characteristic exists in the three developed vertical sections from 1–10 m. Only lithium shows a doubling of the concentration between 5 and 10 m depth (Tab. 1.1).

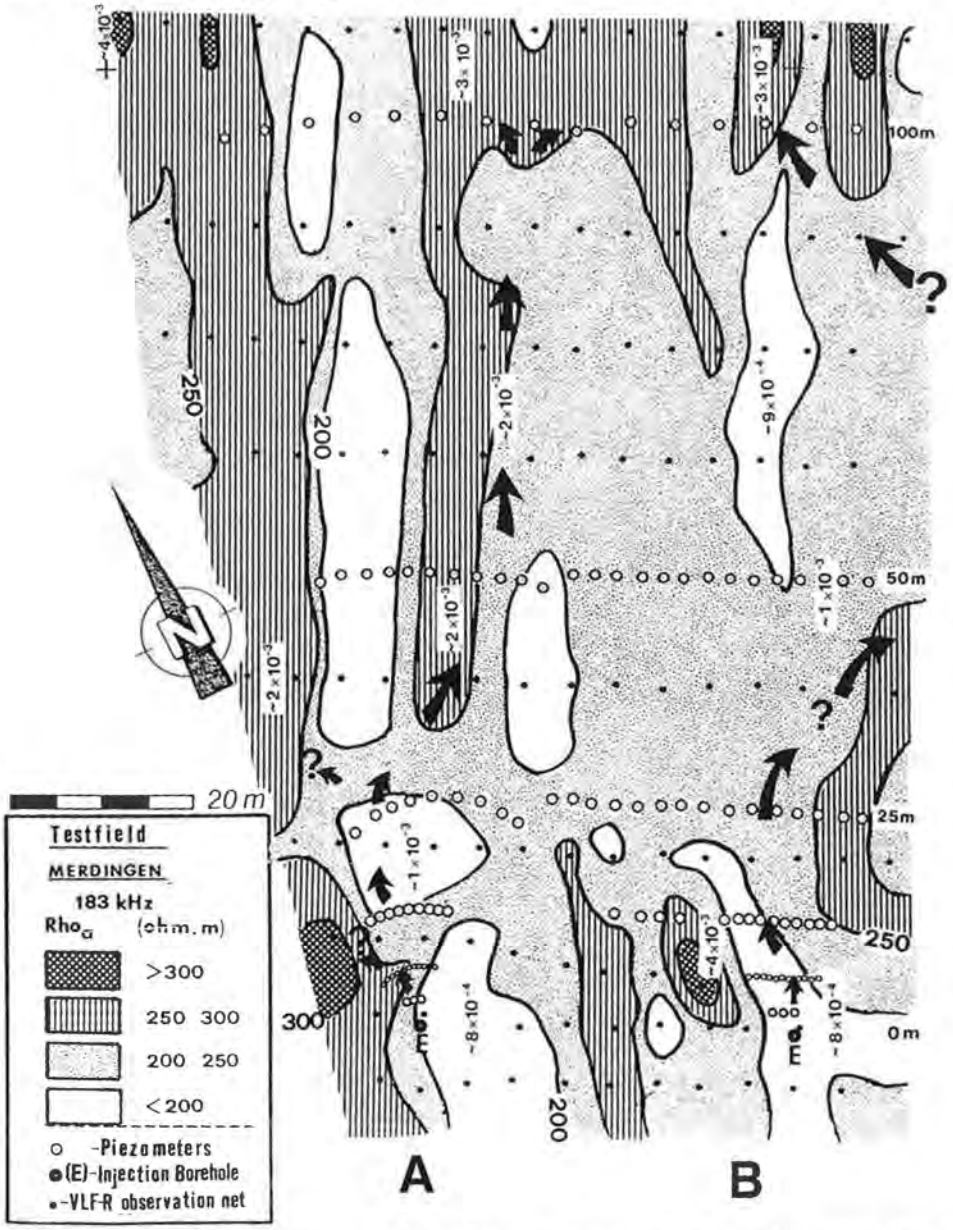

Fig. 1.4: Results of the VLF measurements for the uppermost part of the gravel aquifer of the test area Merdingen (A. DE CARVALHO DILL, W. KÄSS, I. MÜLLER). The figure shows the rows of observation wells of well set A and B, the actual path-arrows, the probable path of the tracer-arrows with questions marks, the most significant permeabilities and the piezometers, which got the greater amount of tracers.

The investigation of isotopes in the three depths doesn't indicate any significant difference (D. RANK). The oxigen-18 values are more or less constant. The tritium concentrations amount about 40 T.U. with a small decrease to the deeper horizon.

Nitrate is subjected to large local and temporal variations in the test field. In the part of the uppermost meter of the aquifer nitrate concentrations could be found between 41 and 102 mg/l through the 38 observation wells on a special reference-day (April 21st, 1985). This varying and comparingly high nitrate concentrations are obviously influenced by agricultural areas in the S, but are mainly due to the decay of plant-material on the surface. Nitrate concentrations between 100 and 550 mg/l were found in the water of the unsaturated zone, in an individual case the concentration was even higher than 700 mg/l (W. KÄSS 1985).

1.4. Geophysical Investigations

Geoelectrical measurements were performed by the "Niedersächsisches Landesamt für Bodenforschung" in the frame of a previous research program. In order to avoid disturbances by the steely observation tubes in the test field the measuring profile was performed some 50 m in the E of the test field in S–N direction. The resistivity of the layers determined by the survey are shown in fig. 1.5. One realizes the irregular stratification of the uppermost layer with a high resistivity between 300 and 900 Ω m, i.e. with a good permeability. Downwards the resistivity of the layers decrease. The range < 100 Ω m is assumed as the bottom layer rich of clay. This layer shows an increasing thickness to the N.

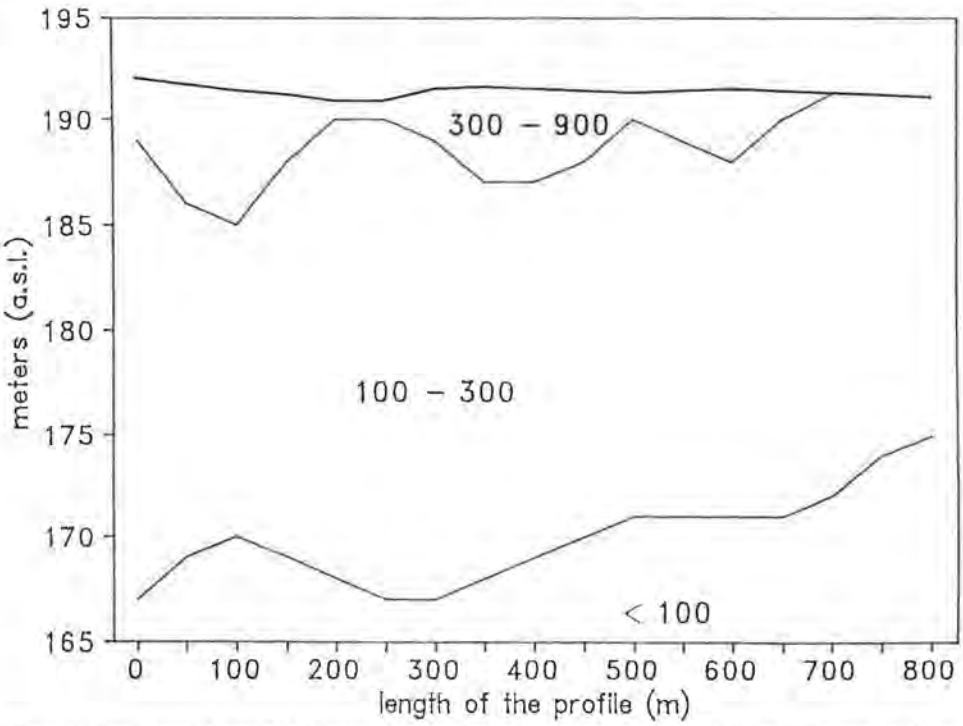

Fig. 1.5: Geoelectrical profile (dotted line in fig. 1.2) from S (0 m) to N (800 m). Ranges in Ω m.

Another geophysical method the **Very Low Frequency-Resistivity (VLF-R)** was applied within the ATH-research program. The object was to get a better knowledge of the underground inhomogeneity of the test area. Beside the evaluation of the sedimentary structures the VLF-R offers an estimation of the hydraulic conductivity of the porous aquifers.

For that purpose the Merdingen test field was covered with nine profiles with a total of 129 points, each in a distance of 5 m (Fig. 1.4). The measurements were carried out on February 10th, 1990. Comparable to the procedure used at the Wilerwald test field three different frequencies were used (183 kHz, 60 kHz and 19 kHz) in order to get also a vertical separation. The dephasing of the electric component of the signal in relation to the magnetic component (Φ) was measured. A description of the principles of the multifrequency VLFR-R vertical sounding, as well as some discussions of the results, can be looked up in "Geophysical Prospecting at Wilerwald Test Field" in the same volume.

Figure 1.4 shows the 183 kHz apparent resistivity contour map with some of the significant permeabiltiy values (in parentheses) for the uppermost horizon. One can notice the marked elongated orientation of the resistivity distribution, which is obviously due to sedimentary structures, like channel fillings.

2. Tracing Experiments (T. Hahn, K. Gerlinger, W. Käss, S. Oetzel, A. Werner)

In the test field of Merdingen 27 tracing tests have been carried out since 1979. The objects were mainly the comparison of different tracers and their suitability for the application in porous aquifers. The main results were published by W. Käss (1985, 1988 and 1990). With regard to different tracers some results are summarized here:

Rhodamine B, injected with a soluted quantity of 100 g into one of the wells on April 6th, 1982, was detectable only in a low concentration in a distance of 75 m about eight months later.

As a matter of fact remnants of Rhodamine B could be found in a visible concentration in the injection point till autumn 1991. During this time the adsorbed Rhodamine B underlay a process of dealcylisation: the fluorescence spectrum shows beside the main peak at 576 nm another one at 519 nm.

For some **Fluorescent Dyes** retardation factors were determined in comparison to Uranine:

R_T Eosine: 1.3
R_T Sulforhodamine B: 1.4
R_T Tinopal CSB-X: 38

Other tests were applied for the transport behaviour of cations. Some relevant R_T-values are listed below – also compared to Uranine (W. Käss, 1990):

Li^+: 1.7
Na^+: 1.2
K^+: 5.1
Rb^+: 36

Cs^{+}: 42
Sr^{2+}: 10
Cd^{2+}: 108

Sodium-Naphthionate, Fluorescent Brightener Tinopal CBS-X and **Leucophor PBS** were less suitable because of their high measuring background in this pore groundwater. Leucophor PBS showed an amazingly low retardation but has a high detection limit of 1 µg/l.

The **Bacteria** of the species *Serratia marcescens* and *Escherichia coli* drifted not further than 50 m. Single germs were still detectable five months after the injection (W. KÄSS et al., 1983).

The **Phages T_4** and **ΦX174** were transported from the injection well with single specimens as far as the 100 m well-row (S. OETZEL et al., 1991).

Fluorescent Microspheres of the size of bacteria though of inaminated material can be used to learn about the transport mechanisms of bacteria. The microspheres were traceable as far as 200 m.

The test field was also used to determine the influence of **Defroster-Chemicals** for runways on the groundwater. Tests were carried out with urea and higher valent alcohols. The former one affected the unsaturated and the saturated zone; the resulting nitrate-increase was recognizable only some meters off because of its high threshold. The higher valent alcohols were decomposed with strong oxigen-demand. Thus the redox-potential of the groundwater was reduced to very negative values with an increased ferrum concentration (W. KÄSS & I. SEEBURGER, 1989).

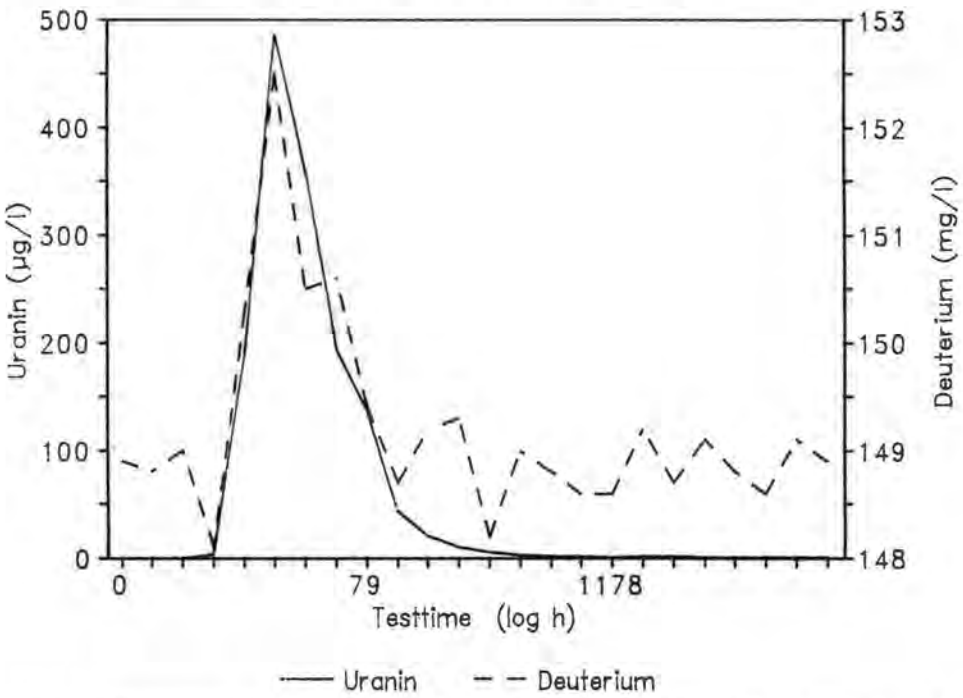

Fig. 2.1: Concentrations of Uranine and Deuterium in a piezometer 6.25 m off the injection borehole (Deuterium measurement by W. STICHLER). The time scale isn't exactly linear!

Two plant-treatment-agents, **Atrazine** and **Terbutylazine**, were injected into the groundwater in small amounts together with Uranine in the eastern test set B. In this test atrazine had a retardation factor of 2.4 compared with Uranine, terbutylazine one of 1.9 (S. KILGER, 1989).

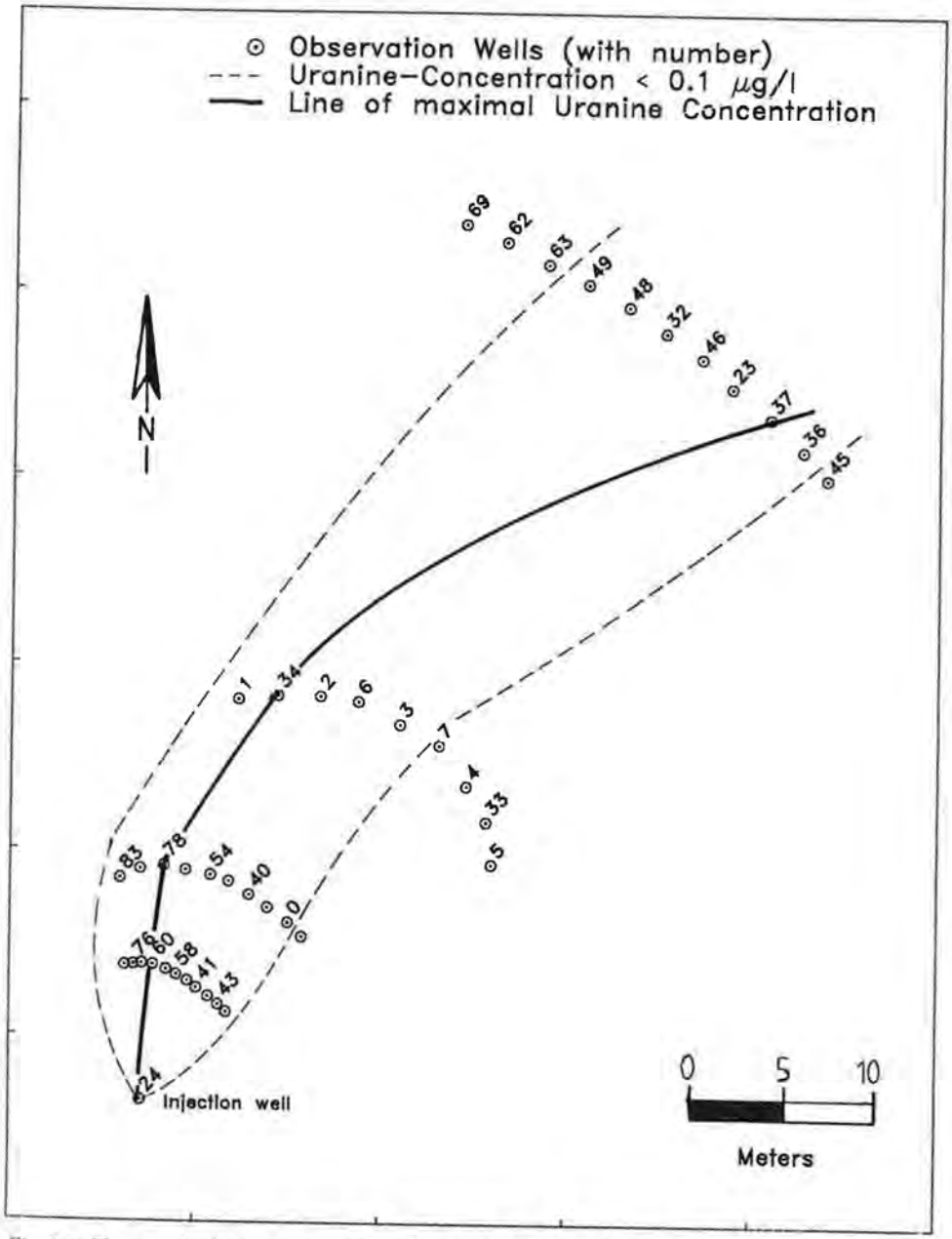

Fig. 2.2: Flow path of Uranine in the well set A of the test field Merdingen. The showed results based on the tracer experiment from April 30th, 1991.

An interesting test was the application of **Heavy Water**. The injection of 330 ml = 334 g D_2O affected an increase of the Deuterium concentration by 7 mg/l after a flow way of 3 m; after a flow way of 6.25 m only by 2 mg/l (Fig. 2.1). Farther away from the injection well Deuterium didn't differ any more from the basic variation. The natural concentration is about 149 ± 1,5 mg/l in the test field. The attainable breakthrough curves ran parallel with the silmultaneously injected Uranine.

B. BARCZEWSKI (1990) successfully applied a newly developed method of the registration of Uranine by the means of optical fibers in the test field,

The last experiment performed in April/May 1991 in the test area of Merdingen (well set A) was a multi tracer experiment with simultaneous injections of Uranine and Strontiumbromide. Figure 2.2 shows the determined path of the tracer Uranine in the front part (up to 50 m distance from injection) of well set A. This experiment was carried out by the ATH-group. Its result served as the main data basis for the evaluation of aquifer parameters by modelling techniques.

The results of the tracer experiments since 1979 especially from the last experiment (Fig. 2.2) are comparable with the measurements with the VLF-R (Fig. 1.4). One can notice:

1) the deflection of tracer transport at the very beginning of its movement (well set A), between both injection points (E) and the 25 m profile line, followed by an inflexion to the right, which can be observed at both sides of the field,
2) a shift to the right (well set B) and possibly evasion of the drawn area, towards more permeable regions. This would explain the non-occurence of tracers at the profile line 50 m (note the presence of the spindle-shaped less permeable structure in fig. 1.4 which would act as deviating barrier) and its reappearance by the 100 m profile line. Figure 1.4 shows the increment of the true resistivity values towards the right hand side just before the 50 m profile line. Nevertheless, it is important not to forget that these resistivity values and consequently the permeabilities correspond to the whole soil column, and that the heterogeneous distribution of permeabilities with the depth is not taken into account.

3. Mathematical Modelling of Tracer Transport

(P. MALOSZEWSKI, A. WERNER)

The quantitative interpretation or simulation of mass (pollutant or tracer) transport in water flowing through groundwater systems requires mathematical description of the processes which may have happened in the system. For more than 30 years dispersion theory introduced by A.E. SCHEIDEGGER (1961) and J. BEAR (1961) has generally been applicable and acceptable as the best one. The convective-dispersive transport equation for conservative tracers (or pollutants) must be coupled with additional equitations describing chemical exchange (ion exchange, sorption-desorption) between liquid (groundwater) and solid (porous matrix) phases in the case of nonconservative tracers. The solution of general transport equation can only be found using numerical methods like finite elements (FEM) or finite difference (FDM). These solutions are mainly applicable to simulate pollutant migration in the case when the transport parameters like space and/or time distribution of water velocity, dispersivities, decay constant and/or chemical reaction constants are already

known. To determine transport parameters the experiments with conservative and reactive tracers have to be interpreted using analytical solutions of simplified (one or two dimensional) transport equation. The tracer experiment from April 30th, 1991 was chosen to determine transport parameters and to compare one dimensional with two dimensional approximations.

3.1. Analytical Solutions for Conservative (Ideal) Tracers

The transport equation of conservative tracer, that are tracers which do not decay or react with the matrix is given for the saturated isotropic porous media by following three dimensional dispersion equation (J. BEAR, 1961):

$$\sum_{l=x,y,z} \frac{\partial}{\partial l} \left(\sum_{k=x,y,z} D_{lk} \frac{\partial C}{\partial k} - v_l C \right) = \frac{\partial C}{\partial t}, \tag{3.1}$$

where

C = the tracer concentration in water, expressed in mass of tracer per unit water volumina;
v_l = the components of water velocity vector in a cartesian coordinate system;
l,k = the cartesian space coordinates;
D_{lk} = the dispersion coefficient, a second rank tensor;
t = the time variable.

Assuming that the cartesian coordinate system is chosen with the x-axis always parallel to the flow direction ($v_x = v$, $v_y = v_z = 0$) and neglecting transversal-vertical dispersion (injection through the whole thickness of aquifer or the observation wells in sufficient distance form the injection well) the eq. (3.1) can be simplified for the homogen system to the from:

$$\frac{\partial C}{\partial t} = D_L \frac{\partial^2 C}{\partial x^2} + D_T \frac{\partial^2 C}{\partial y^2} - v \frac{\partial C}{\partial x}, \tag{3.2}$$

where

D_L = the longitudinal dispersion coefficient;
D_T = the transverse (lateral) dispersion coefficient;
v = the mean water velocity.

A.E. SCHEIDEGGER (1961) assumed that the dispersion coefficients are direct proportional to the water velocity. Neglecting molecular diffusion this results in:

$$D_L = \alpha_L \cdot v, \tag{3.3.1}$$
$$D_T = \alpha_T \cdot v, \tag{3.3.2}$$

where

α_L = the longitudinal dispersivity,
α_T = the transversal dispersivity.

If the tracer experiment is performed simultaneously with the pumping test which produces the radial flow (tracer is injected in the well situated in depression cone) and the concentration of tracer is measured in the water of the pumping well the

transversal dispersion can be neglected according to A. LENDA & A. ZUBER (1970). In this case the transport can be simplified to the one dimensional equation:

$$\frac{\partial C}{\partial t} = D_L \frac{\partial^2 C}{\partial x^2} - v \frac{\partial C}{\partial x}, \tag{3.4}$$

The above equation is also valid for the tracer experiments performed in columns.

In the case of instantaneous injection described by Dirac impuls $\delta(t)$ performed in x=y=0 through the whole thickness H of aquifer the solution to the two dimensional transport eq. (3.2) was given by A. LENDA & A. ZUBER (1970):

$$C(x, y, t) = \frac{M}{nH} \cdot \frac{x}{4\pi v t^2 \sqrt{D_L D_T}} \exp\left[\frac{-(x - vt)^2}{4 D_L t} - \frac{y^2}{4 D_T t}\right], \tag{3.5}$$

where

M = the mass of tracer injected,
H = the thickness of aquifer,
n = the effective porosity (equal to the whole porosity),
x = the distance between injection and detection well measured along the streamline flowing through the injection well,
y = the distance between the streamline exiting from the injection well and the observation well measured perpendiculary to that streamline.

The above solution has three unknown (fitting) parameters: both dispersion coefficients (D_L, D_T) and the mean water velocity (v). These parameters can not be determined simultaneously from the tracer breakthrough curve measured only in one observation well. The inverse problem (finding of transport parameters) can succesfully be solved if the tracer concentrations are observed in several wells situated perpendiculary to the water flow direction. For the well situated on the streamline exiting from the injection well, distance y is equal to zero (y=0) and then the lateral dispersion can be eliminated from eq. (3.5) by normalizing tracer breakthrough curve to the maximal concentration C_{max} measured in that well in time $t = t_{max}$:

$$\frac{C(x, y = 0, t)}{C_{max}} = \left[\frac{t_{max}}{t}\right]^2 \exp\left[\frac{-(x - vt)^2}{4 D_L t} + \frac{(x - vt_{max})^2}{4 D_L t_{max}}\right], \tag{3.6}$$

where

t_{max} = time after injection when the maximal concentration was observed,
C_{max} = the maximal concentration in the observation well.

By using eq. (3.6) the water velocity (v) and the longitudinal dispersivity ($\alpha_L = D_L/v$) can be estimated. To find transversal (lateral) dispersivity the space distribution of tracer concentration along the y-axis for the fixed distance x and for the fixed time t has to be taken into account. The analytical solution describing tracer distribution perpendiculary to the flow direction normalized to the maximal concentration C_{max} is given as:

$$\frac{C(x_{fixed}, y, t_{max})}{C_{max}} = \exp\left[-\frac{y^2}{4 D_T t_{max}}\right]. \tag{3.7}$$

The solution to the one dimensional transport equation for the instantaneous injection in x=0 given by A. LENDA & A. ZUBER (1970) is as follows:

$$C(t) = \frac{M}{Qt_0\sqrt{4\pi P_D (t/t_0)^3}} \exp\left[-\frac{(1-t/t_0)^2}{4P_D\, t/t_0}\right] \tag{3.8}$$

where

t_0 = the mean transit time of water equal to x/v,
P_D = the dispersion parameter equal to D_L/vx,
Q = the pumping rate (discharge).

The above solution can also be normalized to the maximal concentration measured:

$$C(x,t) = \left[\frac{t_{max}}{t}\right]^{3/2} \exp\left[-\frac{1-t/t_0)^2}{4P_D(t/t_0)} + \frac{(1-t_{max}/t_0)^2}{4P_D(t_{max}/t_0)}\right]. \tag{3.9}$$

However in practice it is not necessary to use this solution because in one dimensional case the volumetric flow rate of water through the system or pumping rate Q and mass of tracer enjected M are exactly known and must not be eliminated from the eq. (3.8).

The determination of parameters can be done using automatical best fit method based for example on the least square method (P. MAŁOSZEWSKI, 1981).

3.2. Analytical Solution for Nonconservative Tracers

The transport equation for nonconservative tracers which can react with the porous matrix (ion exchange or sorption-desorption processes) are written for one dimensional case as follows:

$$n\frac{\partial C}{\partial t} + (1-n)\frac{\partial C_s}{\partial t} = n D_L \frac{\partial^2 C}{\partial x^2} - n v \frac{\partial C}{\partial x} \tag{3.10}$$

$$C_s = f(C), \tag{3.11}$$

where C_s is the tracer concentration in the porous matrix, expressed in mass of tracer per matrix volumina. The function f(C), describing the mass transfer of tracer between solute and matrix, has to be defined earlier. In most cases due to its simplicity, the relation (3.11) is defined as a linear function of C:

$$C_s = k_d \cdot C, \tag{3.12}$$

where k_d is the distribution coefficient. Equation (3.12) defines linear exchange model of instantaneous equilibrium. By inserting (3.12) into (3.10) one obtains finally following transport equation:

$$R\frac{\partial C}{\partial t} = D_L \frac{\partial^2 C}{\partial x^2} - v\frac{\partial C}{\partial x}, \tag{3.13}$$

where R is the retardation coefficient. It is equal to:

$$R = 1 + \frac{1-n}{n} k_d. \tag{3.14}$$

The transport of nonconservative tracer which follows linear isotherm reaction with instantaneous equilibrium is R-times delayed in the time domain in comparison to the conservative tracer transport.

In tracer experiment performed in Merdingen, Strontium as an reactive tracer was used. Strontium transport in water flowing through saturated porous sand in the column was modelled by D. KLOTZ et al. (1988). The authors found out that only combined exchange model of instantaneous equilibrium and first order kinetic reaction introduced by D.R. CAMERON & A. KLUTE (1977) can describe the behaviour of Strontium. This combined model was tested in Merdingen to check if it is possible to calibrate the model to the Strontium breakthrough curves found in the field experiment performed under natural flow conditions. The one dimensional transport equation of that model is as follows:

$$\frac{\partial C}{\partial t} = D_L \frac{\partial^2 C}{\partial x^2} - v \frac{\partial C}{\partial x} + \frac{1-n}{n} (\Phi_1 + \Phi_2), \tag{3.15}$$

for the solute phase, where Φ_1 is the tracer flux transfered between solute and porous matrix with linear instantaneous adsorption isotherm:

$$\Phi_1 = \frac{\partial C_{s1}}{\partial t} = k_3 \frac{\partial C}{\partial t}. \tag{3.16}$$

Φ_2 is the tracer flux transfered between solute and porous matrix with linear first order kinetic reaction:

$$\Phi_2 = \frac{\partial C_{s2}}{\partial t} = k_1 C - k_2 C_{s2}, \tag{3.17}$$

where k_1 and k_2 are the forward and backward kinetic reaction rate constants and k_3 is the equilibrium constant for the instantaneous adsorption. C_{s1} and C_{s2} are the tracer concentrations in solid phase (matrix) expressed as mass of tracer per unit matrix volumina. The solution to the above system of equations for the instantaneous injection discribed by Dirac impuls $\delta(t)$ in the entrance to the system (x=0) is as follows (D. KLOTZ et al., 1988):

$$C(x,t) = \frac{M}{Q \cdot t_0 \cdot R_3 \cdot \sqrt{4\pi \cdot P_D \cdot \tau}} \cdot \left\{ \frac{1}{\tau} \cdot \exp\left[\frac{-(1-\tau)^2}{4P_D \cdot \tau} - K_1 \cdot \tau \right] + \sqrt{K_1 K_2 R_3} \cdot \exp(-R_3 K_2 \tau) \cdot \right.$$

$$\left. \cdot \int_0^1 \exp\left[\frac{-(1-u\tau)^2}{4Pd \cdot u\tau} - (K_1 - R_3 K_2) \cdot u\tau \right] \cdot I_1 [2 \cdot \tau \cdot \sqrt{K_1 K_2 R_3 u(1-u)}] \frac{du}{u\sqrt{1-u}} \right\}, \tag{3.18}$$

where

$$R_3 = 1 + \frac{1-n}{n} \cdot k_3, \tag{3.19.1}$$

$$K_1 = \frac{1-n}{n} \cdot k_1 \cdot t_0, \tag{3.19.2}$$

$$K_2 = k_2 \cdot t_0 \tag{3.19.3}$$

are the model parameters expressed in dimensionless variables, and

$$\tau = \frac{t}{R_3 \cdot t_0}, \tag{3.19.4}$$

is a dimensionless time variable. I_1 is the modified Bessel function of the first kind and of the first order. R_3 is the retardation coefficient for instantaneous equilibrium

reaction where as the whole retardation coefficient R_t for both reactions in equilibrium (after ∞ long time) is equal to:

$$R_t = 1 + \frac{1-n}{n} K_d, \tag{3.20}$$

where K_d is distribution coefficient in equilibrium equal to:

$$K_d = k_3 + \frac{k_1}{k_2}. \tag{3.21}$$

The eq. (3.18) describes dispersive-convective transport coupled with combined model of exchange reactions, it consists of five model (fitting) parameters and can not be directly used to solve the inverse problem. To avoid this difficulty the simultaneous injection of conservative and reactive tracer is required. From the breakthrough curve for the conservative tracer the flow parameters (water velocity and longitudinal dispersivity) has to be determined. Their values can later be taken as known parameters in eq. (3.18). It reduces the amount of fitting parameters to the three reaction constants: k_1, k_2 and k_3. The porosity n has to be known or estimated.

4. Results of Modelling (P. MALOSZEWSKI, A. WERNER)

4.1. Conservative Tracers

The purpose of several experiments performed in the test field Merdingen was the qualitative comparison of different artificial tracers. Due to this fact it was necessary to prepare and predict tracer experiment which could be quantitatively interpreted using mathematical models. The main problem was that the injection of tracer had to be performed adequately to the mathematical initial and boundary conditions for which the transport model had been developed. During the last experiment the following aspects were therefore taken into account:

- time duration of injection as short as possible (realization of Dirac impuls);
- simultaneous injection of all tracers (the same hydraulic conditions for the tracers to be compared);
- exact preparation of time schedule of water sampling (exact detection of tracer breakthrough curves including maximal concentrations).

For the planing of the experiment the results of previous tracer tests were used to estimate the mean water velocity and the longitudinal dispersivity. The experimental data collected till present allowed the interpretation of tracer breakthrough curves in the first well rows (6.25–50 m). The quantitative comparison of two "ideal tracers": Bromide and Uranine was only possible for the row in 12.5 m distance from the injection well because of missing Bromide experimental data.

The tracer transport under the natural flow conditions is always a three dimensional process. In practice for determining the transport parameters (solving of the inverse problem) it is not possible to use 3-D numerical solution of transport equation. As it was mentioned in the previous chapter, the two dimensional dispersion model based on the analytical solution of transport equation can be used assuming that the tracer is vertically completly mixed through the whole thickness of aquifer.

The observation wells of the first well rows (up to distance 25 m) catch the tracer plume in the depth till 3 m sufficiently well to apply 2-D model. For the observation wells situated on the main streamline (the well where the maximal lateral concentration in one row – fixed distance x was measured) eq. (3.6) was used to calculate mean water velocity (v) and longitudinal dispersivity (α_L). The tracer breakthrough curves found in those observation wells were additionally interpreted using simple 1-D dispersion model (eq. 3.9). The best fit curves obtained for Uranine in observation well M 34 (x = 25 m) using 2-D and 1-D approximation are shown in fig. 4.1. All results are summarized in tab. 4.1. Both models fit the tracer breakthrough curves

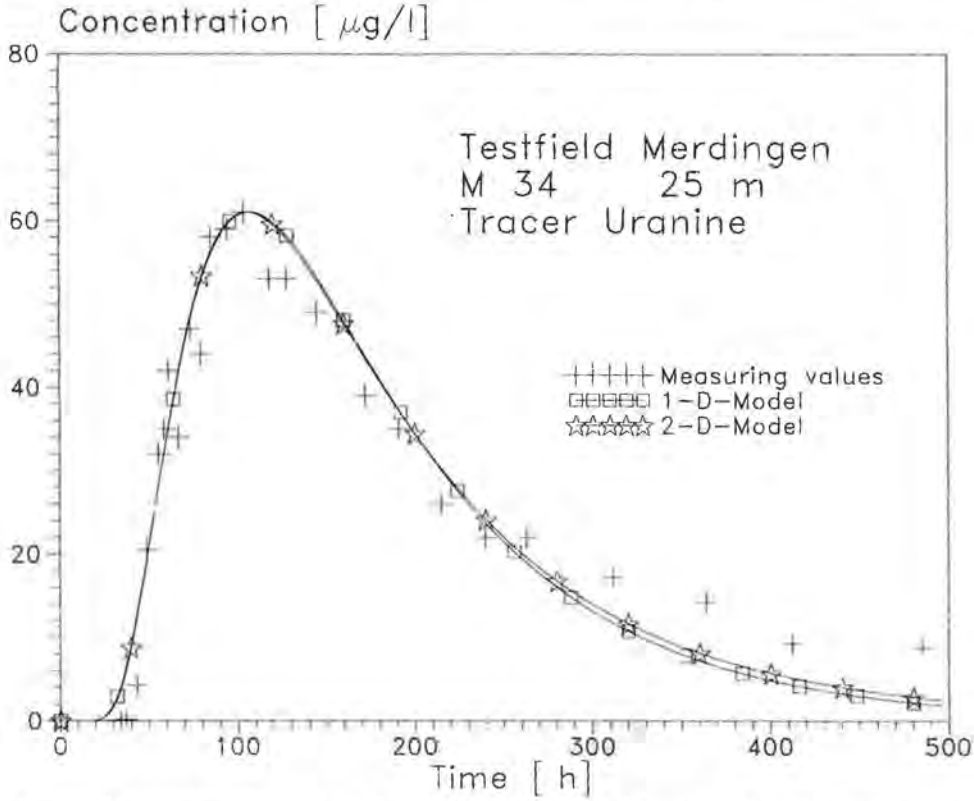

Fig. 4.1: The comparison of the best fits obtained by using 1-D and 2-D transport models to the Uranine concentration curve.

Tab. 4.1: Results of the interpretation of Uranine breakthrough curves with the 1-D and 2-D dispersion model.

Observation well	Distance [m]	α_L [m]		v [m/d]	
		1-D	2-D	1-D	2-D
M 58	6.25	0.46	0.46	22.5	21
M 54	12.5	3.6	2.8	3.9	5.3
M 34	25	4.6	5.2	3.4	2.6
M 37	50	6.6	7.2	2.9	2.4

with nearly the same accuracy. More exact 2-D model produces nearly in all cases smaller water velocities and higher longitudinal dispersivities. The water velocity found for the distances x = 6.25 m and 12.5 m is remarkably high (21 and 5.3 m/d, respectively) and not representative for the natural flow conditions in the test field (s. fig. 4.2). It is due to the fact that the injection well was flushed too long with the clean water producing high gradient. The differences in transport parameters are neglectably small for the first row and increase with the flow distance (for x = 50 m – the difference in the water velocity is about 20% and that of dispersivity about 9%). It is necessary to point out that the parameter values obtained for the different rows are the average mean values for the flow distance between injection and observation wells.

The transversal dispersivity (α_T) was determined using eq. (3.7) from the lateral space distribution of tracer plume. The mean value of α_T was found to be about 0.06 m. The example of best fit curve for the transversal distribution of Uranine is shown in fig. 4.3.

The parameters obtained for two tracers Uranine and Bromide using 2-D dispersion model are summarized in tab. 4.2. The Uranine in comparison to Bromide, has shown about two times greater dispersivity and two times lower velocity. It may suggest probable sorption of Uranine in the groundwater system under consideration.

From the water velocity v = 2.36 m/d and natural gradient i = 0.0006 taken between rows in the distances 50 and 25 m, one obtains respectively for assumed effective

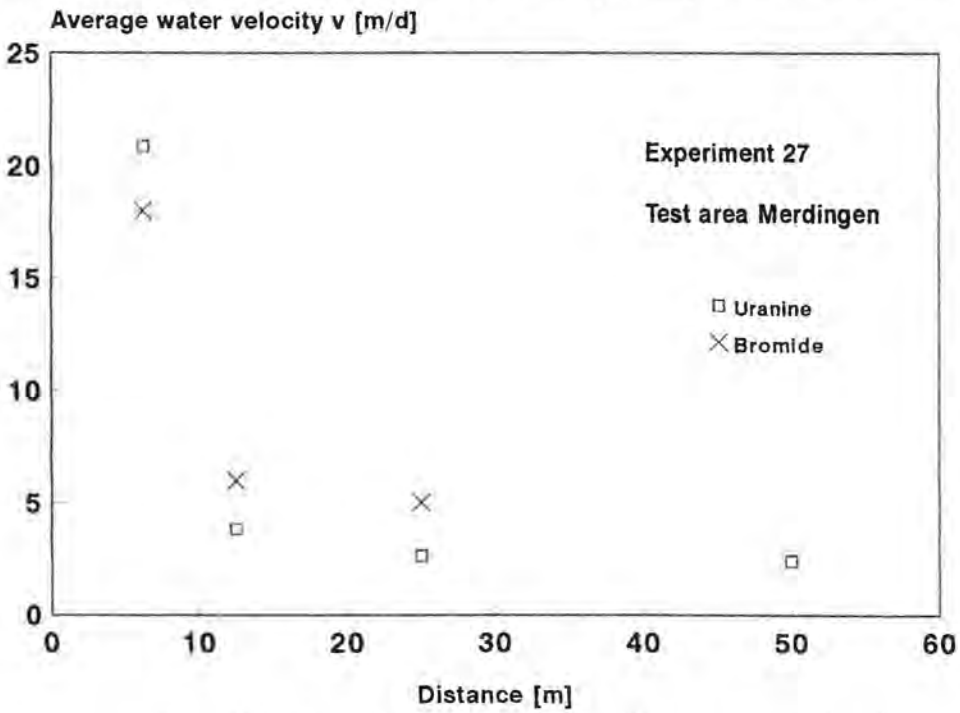

Fig. 4.2: Mean flow velocity found from Uranine and Bromide curves measured in the main observation points of the well rows of the test area Merdingen (2-D model). The results based on flow distances calculated for a streamline connected the injection well with the observation point.

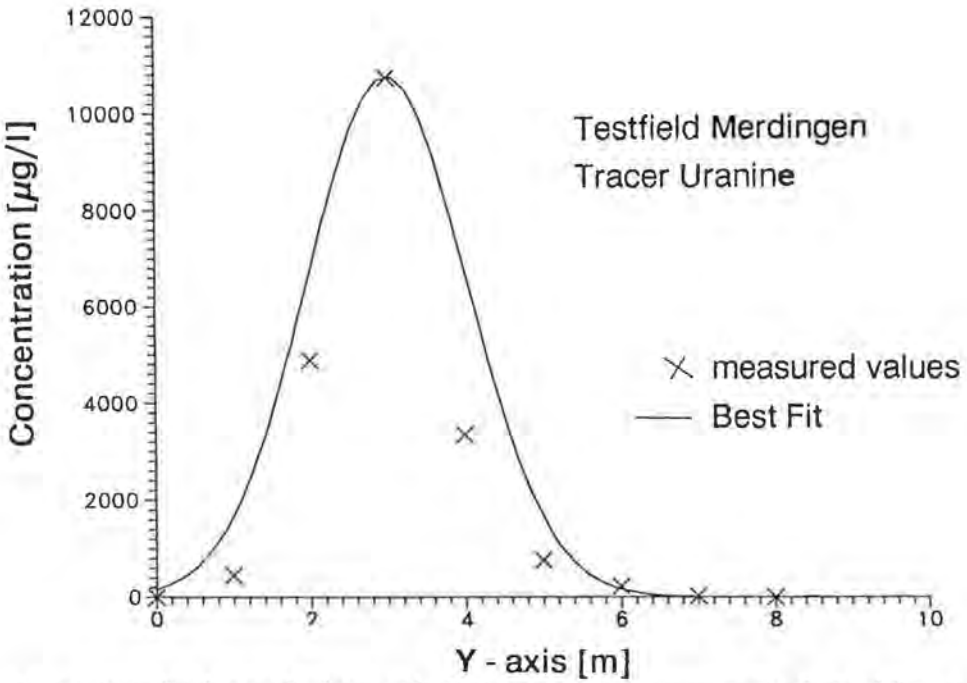

Fig. 4.3: Space distribution (fixed time: 31 h after injection) of tracer concentration for fixed distance x = 12.5 m with fittings after eq. (3.7). The determined transverse dispersivity value is $\alpha_T = 0.06$ m.

porosity of n = 0.25, the mean hydraulic conductivity $k_f = 1.1 \times 10^{-2}$ m/s. The k_f value is about five times higher that the k_f value found from the VFL measurement but its accuracy strongly depends on the exactness of water heads measurements. Simultaneously, the geophysical method yields the mean weighted k_f up to the depth of about 20 m, whereas the tracer data are related in considered case only to about 5 m.

Tab. 4.2: Calculated flow and aquifer parameters for the tracers Uranine and Bromide.

Observation well	Distance [m]	α_L [m]		v [m/d]	
		Uranine	Bromide	Uranine	Bromide
M 54	12.5	3.6	1.6	3.9	6
M 34	25	4.6	1.8	3.4	4.8
M 37	50	6.6	–	2.9	–

4.2. Nonconservative Tracers

The comparison of the flow parameter (Tab. 4.1) shows that the difference between the 1-D and the 2-D model are very small.

Therefore the 1-D-transport model for nonconservative tracers (eq. 3.10) can approximatly be used for the interpretation of the reactive tracer Strontium.

For combined model of instantaneous equilibrium and first order kinetic reaction one obtains the analytic solution given by eq. (3.18). Figure 4.4 shows a best fit of a theoretical Strontium curve to the concentrations measured.

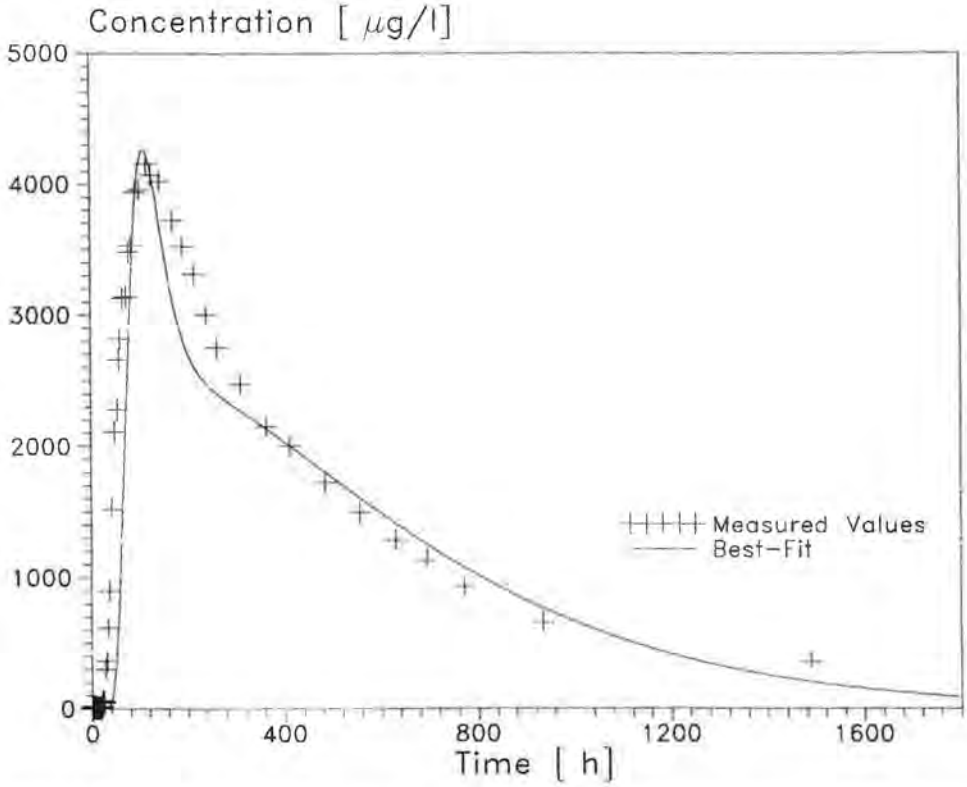

Fig. 4.4: Strontium concentration curve obtained as a best fit to the values measured in the observation well 55, by using combined model (eq. 3.18) with $k_1 = 0.40\ d^{-1}$, $k_2 = 0.13\ d^{-1}$ and $k_3 = 0.9$. The water velocity $v = 7.4$ m/d and dispersivity $\alpha_L = 0.9$ m calculated from Bromide based on 1-D model.

The maximal area of the breakthrough curve as well as its tailing can be described with this model. Table 4.3 shows the determined parameter values for some observation wells of the test field. Because of missing Bromide datas of the wells in greater distance, it is not possible to find the parameter for increasing distance from the injection well.

Tab. 4.3: Results of the interpretations of the Strontium breakthrough curves with the combined model of exchange reactions (3.18).

Observation well	Distance [m]	t_0 [h]	P_D [ ]	k_1 [1/d]	k_2 [1/d]	k_3 [ ]	K_d [ ]
M 78	12.5	44	0.1	0.3	0.10	0.3	3.3
M 55	12.5	41	0.1	0.4	0.13	0.9	4.0
M 54	12.5	28	0.1	0.6	0.11	0.5	6.0

The analytical solution (3.18) was until now only used for the interpretation of column experiments (in laboratory). In this case, the application of combined model in field experiments yields also comparable results with those obtained by D. KLOTZ et al. (1988). For further signification of the model more experiments with Strontium and others reactive tracers need to be performed and interpreted.

5. Interpretation of Tracer Experiments with a Numerical Model (K. GERLINGER)

5.1. Numerical Model

The analytical solutions represent one mathematical method to solve the partial differential equations which describe the transport of a dissolved contaminant in the subsurface. Their application is limited to cases with steady-state flow, e.g. flow with a constant velocity in time and space. Homogeneity and isotropy within the whole test area is required.

The numerical models, on the other side, replace the partial derivatives appearing in the differential equations by algebraic equations. These constitute a system of linear equations that has to be solved for the required variables. The algebraic equations are obtained by dividing the continuum which makes up the region into a finite number of blocks. As each block has its own hydrogeologic properties, it is possible to include heterogeneity (e.g. variation of the flow field) in the model. All blocks are connected by the law of continuity. To solve the algebraic equations, the numerical models require a detailed definition of the initial and boundary conditions (e.g. the hydraulic heads at the boundaries of the model area).

Numerical groundwater models first solve the flow equation to obtain the hydraulic head distribution h(x,y,t). Applying Darcy's law, the hydraulic heads are used to calculate the pore velocity v(x,y,t) which is necessary to solve the transport equation. Figure 5.1 shows the governing equations for the transport modelling together with the required parameters and explains their relationship. Modelling software usually combines flow and transport equations. The analytical solutions, on the contrary, solve each equation by itself. Using the analytical solution, the pore velocity can be inserted directly into the transport equation while the numerical model calculates the velocity from the simulated head distribution.

The two dimensional groundwater model MOC was used for the numerical evalution of the Uranine tracer test in the test area. This program is distributed by the International Groundwater Modelling Center, Indianapolis (L.F. KONIKOW & J.D. BREDEHOEFT, 1978). For this investigation the version 3.0 (D.J. GOODE & L.F. KONIKOW, 1989) was available at the Institut für Wasserbau, Stuttgart (Prof. Dr. G. TEUTSCH).

In its original version, the MOC program enables only a transport grid consisting of 20×20 blocks.

The model area can only be spatially discretized into rectangular blocks of constant dimensions. With this mesh size, an evaluation of the tracer curves of the test area is impossible, because some blocks contain more than one measuring point. The program was transferred to the IBM mainframe 3090 to enable an extension of the number of blocks to 70×70.

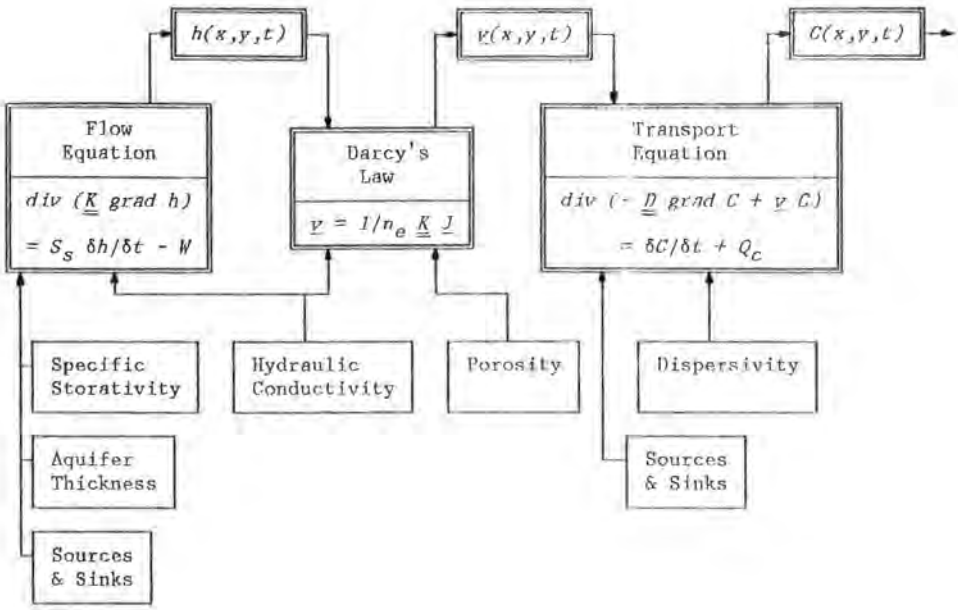

$\underline{\underline{K}}$: hydraulic conductivity tensor $[L/T]$
h : hydraulic head $[L]$
S_s : specific storage $[1/L]$
W : injection or withdrawal of a water volume per unit time and per unit volume $[1/T]$
$\underline{v}$: pore velocity vector $[L/T]$
n_e : effective porosity $[\ ]$
$\underline{J}$: hydraulic gradient vector $[\ ]$
$\underline{\underline{D}}$: dispersion tensor $[L^2/T]$
C : concentration of the dissolved contaminant $[M/L^3]$
Q_c : sources or sinks $[M/L^3T]$
grad A : gradient of a scalar A (grad $A = \delta A/\delta x,\ \delta A/\delta y,\ \delta A/\delta z$)
div A : divergence of a vector A (div $A = \delta A_x/\delta x + \delta A_y/\delta y + \delta A_z/\delta z$)

Fig. 5.1: Equations of contaminant transport.

In the MOC program, the flow equation and Darcy's law are solved by the finite difference method. Using this method, the derivatives in the differential equations are replaced by the difference between discrete points.

The method of characteristics is used for the numerical solution of the transport equation. This method breaks up the transport equation into two parts, one accounting for advection and the other accounting for dispersion. Each part is solved separately.

5.2. Analysis of the Hydraulic Heads

A detailed knowledge of the head distribution in the model area is a prerequisite for the calibration of the numerical model. Measurements of the hydraulic heads in the test area were carried out and showed small-scale differences within the measuring rows.

Figure 5.2 shows a representative picture of the hydraulic heads on April 28th, 1991, shortly before the tracer test. The lowest heads in the two measuring rows closest to the injection point are located more to the left side of the respective row. This corresponds to the direction of preferential tracer transport as determined in the experiment. In the 25 m-row the differences of the measured heads are small. In the 50 m-row and in the 100 m-row low water levels can be seen to the right side of the rows. At these points high tracer concentrations were measured during the test. The lowest hydraulic heads in the 50 m-row and 100 m-row are to the left side. There, another tracer breakthrough could be expected but no samples were taken at these points.

Interesting is a comparison of the pattern of hydraulic heads with the results of the VLF-R measurements. The locations of the measuring points with the lowest water level correspond to the areas of higher permeability in fig. 1.4. This indicates that the small-scale variability of the groundwater levels is due to varying permeabilities in the subsurface. An elevated groundwater level in a piezometer originates from a local water build-up due to a reduced permeability, whereas a low water level is a sign for higher permeability.

The detailed measurements of the hydraulic heads can therefore be used to obtain the possible distribution of hydraulic conductivities. As the tracer moves according

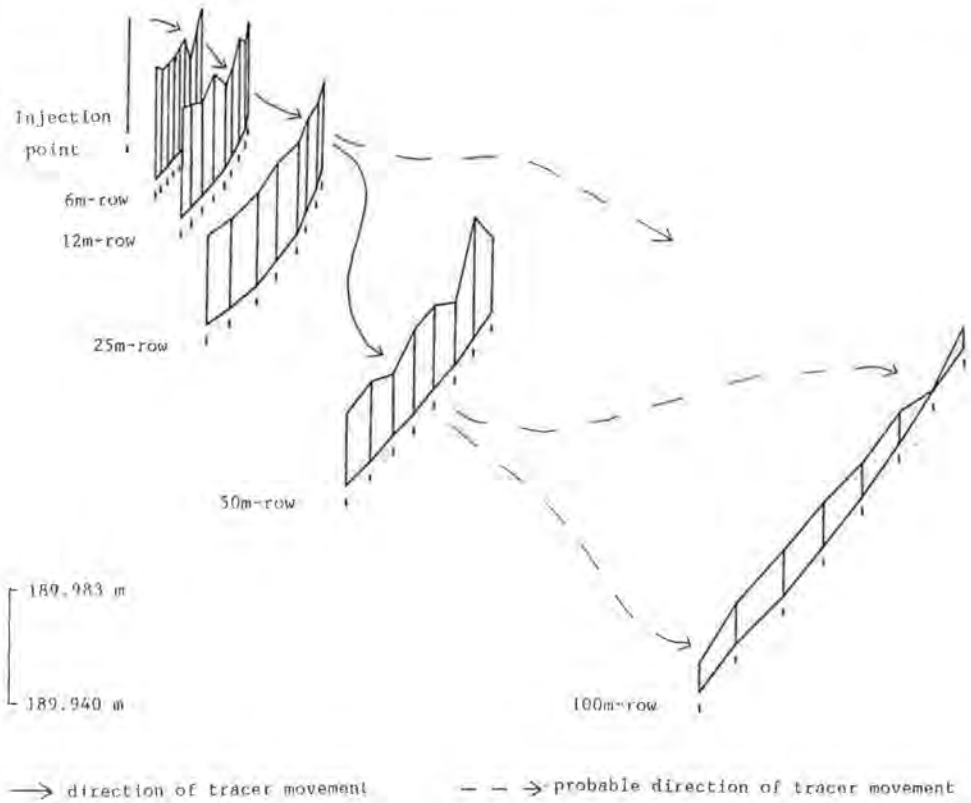

Fig. 5.2: Hydraulic heads in the test field on April 28th, 1991. The length of the bars indicates the hydraulic head at the respective measuring point.

to the varying permeabilities in the subsurface, measurements of the hydraulic heads can also indicate preferential pathways for tracer transport.

5.3. Application of the Numerical Model

5.3.1. Validation of the Model by Varying the Hydraulic Conductivity

The measurements of the groundwater levels did not show a time-dependent variability of the hydraulic heads. For this reason a steady-state case is assumed to facilitate the calculation. The hydraulic head measurement of a set date are used for the steady-state calibration. The spatial variability of the groundwater level is simulated by varying the hydraulic conductivity in the model grid.

The hydraulic head distribution determines the pore velocity which is not only important for the advective transport but influences the dispersive spreading as well. The pore velocity is the most sensitive parameter of a groundwater model.

To start the simulation a basic model of the test area is created. The boundaries of the groundwater inflow and outflow of the groundwater are determined as a constant head boundary condition. This means that the hydraulic heads in the first and last cell row, along the part of the boundaries that is perpendicular to the flow direction, remain unchanged during the simulation. A hydraulic gradient of 0.04% is specified, according to the measurements of the groundwater levels.

The constant head boundaries have a strong influence on the result of the flow modelling. A calibration which only considers constant head boundary conditions always leads to a plausible head distribution. Due to that, it is also necessary to check the inflow and outflow of the model area. In general, preference should be given to a calibration that refers to the water balance. However, the information necessary to perform a water balance is mostly not available.

This is also the case for the test field Merdingen. There is a lack of information about the thickness of the aquifer. A determination of the inflow and outflow of the aquifer is therefore impossible. Additionally, there are no measurements of the water levels to the sides of the injection point through which the inflow into the area takes place.

By varying the values of the hydraulic conductivity in the cells an attempt is made to simulate the small-scale variability of the groundwater levels. The numerical model responds to an increase in permeability in a certain area with a relatively low water level in those cells of this area which are the closest to the inflow boundary. The hydraulic head then remains on the same level over the rest of this area and hardly decreases. In consequence there is, compared to the case without increase of the permeability, a reduced hydraulic potential between a cell at the inflow boundary and the last cell of the area with higher permeability.

The reason for this response is that the program also considers the mass balance. Increasing the permeability in an area without changing the hydraulic gradient is equal to a higher flow through the model area. Since there are no sources or sinks in the area this is impossible and a variation of the permeability must cause a variation of the gradient into the opposite direction. In the numerical model, an area with higher permeability which would normally result in an increased flow shows a reduced gradient and therefore the flow remains the same. This does not correspond to the measurements of the groundwater levels and the results of the VLF-R

measurements which found higher hydraulic gradients in the measuring rows of the more permeable areas.

Additionally, the hydraulic heads in a cell in the numerical model are calculated using the hydraulic heads of the respective neighbouring cells. This creates a relatively smooth groundwater level distribution. Cells with a lower permeability neighbouring more permeable areas show nearly identical water levels. The small-scale variation of the groundwater levels as they are documented by the measurements cannot be simulated by the model.

As it is impossible to model the groundwater flow field using the water level data, the results of the tracer tests were used to calibrate the flow. The most important information for contaminant transport is not so much the exact values of the hydraulic heads in the cells but the average transport velocity. The analytical solution gives values for the pore velocities in the test area.

The evaluation of tracer experiments in the test field Merdingen with the analytical solution shows that the pore velocity in the area of the 50 m and 100 m-rows is about 2 m/d. To simulate a velocity of 2 m/d in all cells of the numerical model, constant values for the hydraulic conductivity, the porosity and the dispersivity were specified. In the next step, an augmentation of the hydraulic conductivities in a block which represents the first two measuring rows is done to simulate the analytically determined velocity of about 10 m/d.

However, the increase of the permeabilities in the area close to the injection cell by two orders of magnitude can only triple the calculated velocities. Even higher permeabilities result in no further increase in velocity but in an error in the calculated mass balance. Only the reduction of the size of the area of elevated permeabilities leads to an increase in velocity.

Since it is necessary to keep the mass balance, it is impossible to obtain the desired velocities by defining a block with high permeabilities. By specifying the velocity in the back part of the model grid at 2 m/d the outflow out from the model area is fixed. As the mass balance has to be kept, it is impossible to have a block of the supposed size with velocities of about 10 m/d because this implies higher inflow across the model boundary.

Due to the conditions in the test field Merdingen the variation of the hydraulic conductivities can neither simulate the measured heads nor the determined velocity. Therefore, the calibration of the program was done by varying the porosity per cell. The porosity has a linear relationship to the computed pore velocity but is not related to the hydraulic gradient. Theoretically, this allows the simulation of any pore velocity. With the MOC program it is only possible to define a constant porosity for all cells . By changing the source code of the numerical model a specification of the porosity per cell was enabled.

5.3.2. Calibration of the Model by Varying the Porosity

To achieve the measured hydraulic gradient of 0.04% in the numerical model, constant head conditions and a constant hydraulic conductivity for the whole area were chosen. Varying porosity values result in varying pore velocities. Computed tracer breakthrough curves, using those velocities, are then compared with the curves of the tracer test. This comparison yields a value for the porosity, which is directly related to the initial choice of the hydraulic conductivity. This means, that when e.g. doubling the hydraulic conductivity the porosity can be divided by two to result

in the same velocity. For this reason, only the ratio between hydraulic conductivity and porosity makes sense as a result.

This result, however, is not unique. It can be shown, that two different velocities within an area can also be represented by an average velocity, with the same final result. Velocities could be chosen rather arbitrarily and their combination could still simulate the spatially varying measured velocity.

Using a constant hydraulic gradient could not explain the movement of the tracer plume towards the right side of the area around the 50 m-row. The constant gradient causes a movement into one fixed direction only. The model can then only simulate lateral transport by lateral dispersion which is considerably less. For this reason the calibration was performed without the 50 m-row.

Ideally, it should be possible to model breakthrough curves by only varying the velocities because dispersion, too, is a result of velocity gradients. If one could reduce the cell size to the degree that each change of the velocity vector, length or direction, could be documented, the transport equation could be written without the part that describes dispersion. But the velocity changes on a microscopic scale which cannot be detected nor can one reduce the cell size indefinitely since computer memory is limited. In the test field Merdingen, the simulation of the breakthrough curves is impossible if only the porosity (and by that the velocity) is varied. The shape of the breakthrough curves can only be modelled when using varying values of dispersivity in the model area. The MOC program was modified in a way that the dispersivity can be defined separately for each cell. The magnitude of the longitudinal dispersivity can be estimated from the analytical solution. The ratio of longitudinal to lateral dispersivity is assumed to be 10%.

5.3.3. Results of Simulation

Figure 5.3 shows the determined values for the dispersivity and for the ratio of hydraulic conductivity and porosity. The breakthrough curves that were created by the numerical model, using these values show satisfying accordance with the measured curves. The pore velocities can be computed by multiplying the ratio of hydraulic conductivity and porosity by the hydraulic gradient.

It can be seen that the pore velocities are high close to the injection point and that they decrease considerably towards the back part of the area. An explanation for this velocity distribution could be the conditions of the tracer injection. The sampling well was rinsed before and after the tracer injection. The injection of water into the aquifer increases hydraulic head and pore velocity at the injection site and could result in an accelerated tracer movement.

Another reason for the velocity distribution could be a high permeability layer at the top of the aquifer where the tracer moves faster. Such a layer could explain the fast movement of the tracer near the injection point without violating the water balance of the area. As the water balance of a two dimensional flow model considers the flow across the whole aquifer thickness it is impossible to simulate different vertical layers. A complete simulation would require a three dimensional model.

The analytical solution allows to separately evaluate each measured breakthrough curve. The results are not automatically combined to represent the overall hydrogeologic conditions. The numerical model, however, uses information of the whole area where all measurements lead to a comprehensive model for the considered region. For this reason the breakthrough curves of the numerical model do not match as

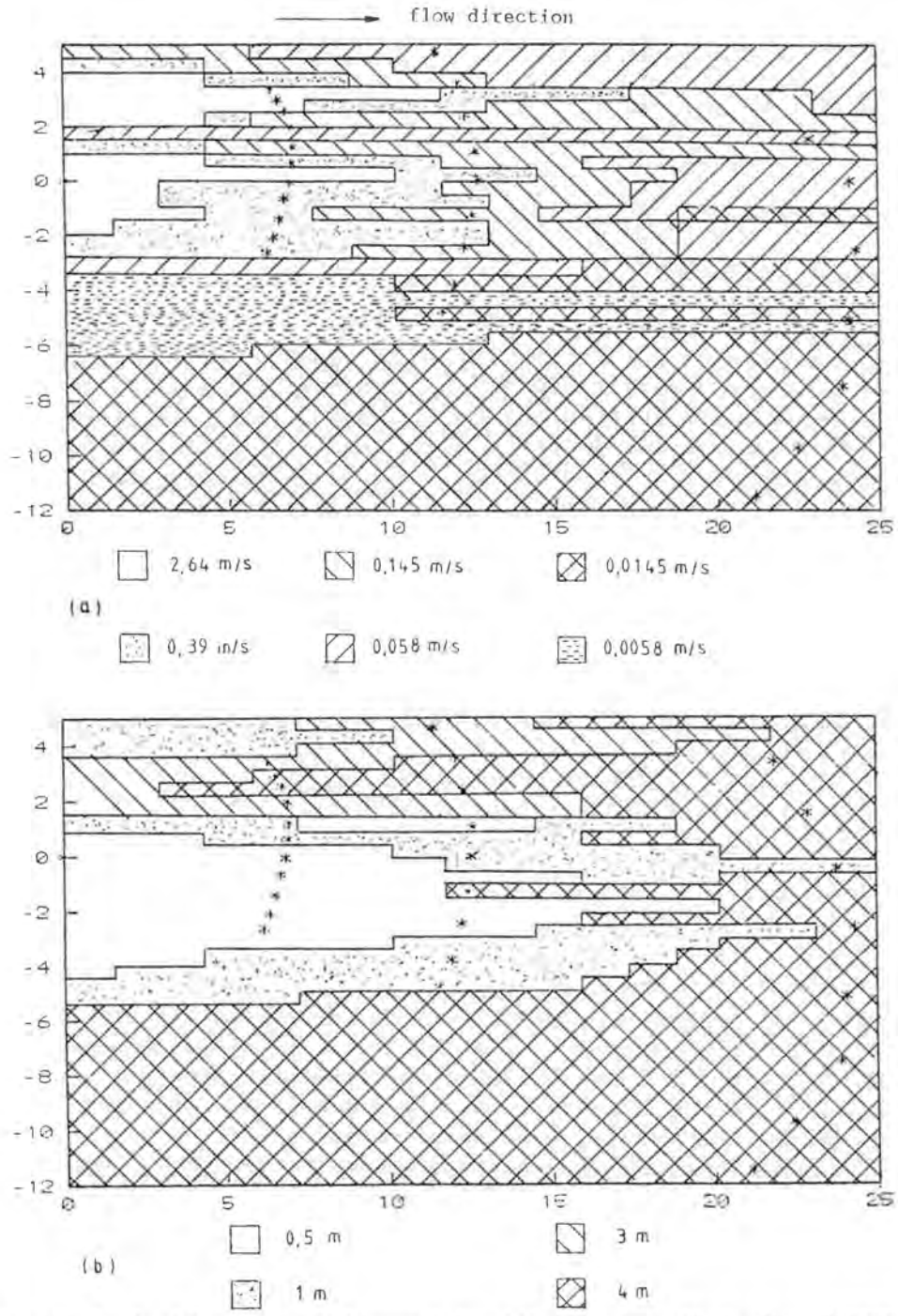

Fig. 5.3: Results of the validation of the numerical model for (a) the ratio of hydraulic conductivity and porosity and (b) the dispersivity. The axes indicate the distance from the injection point in meters.

accurately as when evaluated separately by the analytical method. As shown before in the simulation of the water levels it is often difficult to accurately describe the small-scale variability of natural systems by a model.

Modelling averages away the details of the natural system. Thus, numerical models are more suitable to simulate average concentrations and the distribution of contaminants on a larger scale.

6. Conclusions (A. De Carvalho Dill, K. Gerlinger, T. Hahn, H. Hötzl, W. Käss, Ch. Leibundgut, P. Maloszewski, I. Müller, S. Oetzel, D. Rank, G. Teutsch, A. Werner)

A test field in a porous aquifer offers numerous possibilities to test the behaviour of tracers of any kind in groundwater in surveyable time spaces. Even harmful substances can be investigated if little injection amounts are used. The realization of the groundwater qualities as well as hydrogeological, geophysical and petrological investigations belong to a general view.

The VLF-R method revealed the existence of an elongating distribution of permeabilities which acting as a force of attraction (the more permeables ones) or as a deviating barrier (the less permeable ones) results in preferential paths of tracer transport. This feature is in accordance with the results of many previous tracer tests.

The interpretation of tracer experiments and the determination of the parameters dispersivity and velocity is possible with the analytical solutions of the dispersion equation. In the test field Merdingen the comparison of 1-D and 2-D models shows that the deviation is only small. Higher difference one can get by comparison of Uranine and Bromide. Bromide is with regard to its transport properties the more ideal tracer.

Based on the received flow velocity one can get the mean hydraulic conductivity. Differences to the values after VLF-R method are mostly founded on the uncertainty by the determination of the hydraulic gradient.

The extension of the dispersion model with exchange reactions enables to describe nearly exact the sorption processes of the reactive tracer Strontium.

The application of the numerical model shows that it is difficult to simulate the small-scale variability of the hydrogeologic conditions. As the model averages away the details, it should be used preferentially to describe average concentrations of contaminants.

The advantage of the numerical groundwater model is its flexibility. This allows the inclusion of more aspects, e.g. insteady-state flow, pumping wells or heterogeneity of the area. With such a comprehensive model, it is possible to simulate different scenarios under various conditions.

References

Barczewski, B. (1990): Optische Methoden zur in-situ Tracerkonzentrationsmessung. – Wasserwirtschaft, 80 (11), 553–561.

Bear, J. (1961): On the Tensor Form of Dispersion in Porous Media. – Journal of Geophysical Research, Vol. 66, No. 4, 1185–1198, Washington D.C. (U.S.A.).

CAMERON, D.R. & A. KLUTE (1977): Convective-Dispersive Solute Transport with a combined equilibrium and kinetic adsorption model. – Water Resour. Research, **13** (1), 183–188, Washington D.C. (U.S.A.).

GOODE, D.J. & L.F. KONIKOW (1989): Modification of a Method-of-Characteristics Solute-Transport Model to Incorporate Decay and Equilibrum-Controlled Sorption or Ion Exchange – U.S. Geological Survey Water-Resources Investigations Report 89-4030, Reston (Virginia).

KÄSS, W. (1985): Chemische Transportmechanismen in der Ungesättigten Zone. Untersuchung mit Markierungsmitteln. – Z. dt. geol. Ges., **136**, 481–496, Hannover.

KÄSS, W. (1988): Markierung von Porengrundwasser. – Proc. 5th Intern. Symp. Underground Water Tracing (SUWT) 1986, 191–201, Athens.

KÄSS, W. (1990): Chemiesorption als natürliche hydrologische Barriere. – Z. dt. geol. Ges., **141**, 225–231, Hannover.

KÄSS, W., R. RITTER & C. SACRE (1983): Lebensdauer und Transport von Bakterien in typischen Grundwasserleitern – Oberrheinische Schotterebene. – DVGW-Schriftenreihe Wasser, **35**, 127–138, Eschborn.

KÄSS, W. & I. SEEBURGER (1989): Redoxpotential-Messungen im Grundwasser. – DVWK-Schriften, **84**, 1–118, Hamburg/Berlin.

KILGER, S. (1989): Fallstudie zur Grundwasserbelastung durch Nitrat und s-Triazine in einem landwirtschaftlichen Einzugsgebiet. – Unveröff. Diplomarbeit, 105 p., Trier.

KLOTZ, D., P. MALOSZEWSKI & H. MOSER (1988): Mathematical Modelling of Radioactive Tracer Migration in Water Flowing through Saturated Porous Media. – Radiochimica Acta, **44/45**, 373–379, München.

KONIKOW, L.F. & J.D. BREDEHOEFT (1978): Computer Model of Two-dimensional Solute Transport and Dispersion in Ground Water – U.S. Geological Survey Techniques of Water Resources Investigations, Book **7, C2**.

LENDA, A. & A. ZUBER (1970): Tracer dispersion in groundwater experiments. – Isotope Hydrology **1970**, 619–642, IAEA, Vienna.

MALOSZEWSKI, P. (1981): Computerprogramm für die Berechnung der Dispersion und der effektiven Porosität in geschichteten porösen Medien. – GSF-Bericht **R 269**, GSF München/Neuherberg.

MELU & MWMV – MINISTERIUM FÜR ERNÄHRUNG, LANDWIRTSCHAFT UND UMWELT, MINISTERIUM FÜR WIRTSCHAFT, MITTELSTAND UND VERKEHR (Ed., 1977): Hydrogeologische Karte Baden-Württemberg, Kaiserstuhl – Markgräflerland. – 65 p., 6 Karten 1 : 50,000, 8 Anlagen, 7 Tabellen, Freiburg.

NLfB – NIEDERSÄCHSISCHES LANDESAMT FÜR BODENFORSCHUNG (1982): Bericht über geoelektrische Untersuchungen bei Merdingen, Kreis Breisgau – Hochschwarzwald v. 8. April 1981. – Archiv-Nr. 88109, 4 p., 3 Anl., 24 Sondierprofile, Hannover.

OETZEL, S., W. KÄSS, T. HAHN, B. REICHERT & K. BOTZENHART (1991): Field experiments with microbiological tracers in a pore aquifer. – Water Sci. Tech., **24** (2), 305–308.

SCHEIDEGGER, A.E. (1961): General Theory of Dispersion in Porous Media. – Journal of Geophysical Research, Vol. **66**, No. **10**, 3273–3278, Washington D.C. (U.S.A.).